QUASI-ELASTIC NEUTRINO SCATTERING*)

R.L. Kustom, D.E. Lundquist, T.B. Novey and A. Yokosawa

Argonne National Laboratory,
Argonne, Illinois, U.S.A.

F. Chilton

Stanford Research Institute,
Menlo Park, California, U.S.A.

ABSTRACT

Quasi-elastic scattering of neutrinos, $\nu + n \rightarrow p^+ + \mu^-$, was measured in a 30 ton spark chamber detector. Analysis of the cross section versus momentum transfer yields a value of $M_{A_1} = 0.7 \pm .15$ for a single pole type axial-vector form factor or $M_{A_2} = 1.05 \pm .2$ for a double pole form factor. No decrease in cross section at low momentum transfer expected due to nuclear effects was observed.

We have studied the quasi-elastic scattering of neutrinos, by the reaction $\nu + n \rightarrow p^+ + \mu^-$ in a neutrino beam prepared in the external proton beam of the Argonne Zero Gradient Synchrotron. The detector was a 30-ton assembly of steel plates and spark chambers previously described.[1, 2, 3]

Top and side views of the apparatus are shown in Figure 1. The neutrino beam is prepared via the ZGS fast extraction system.[4] 50% of the circulating proton beam was extracted in about 50 microseconds. A beryllium target, 3 cm. in diameter and 60 cm. long, was located in a current sheet focusing horn[5] pulsed to a current of 150 kiloamperes. The horn is followed by a 50-foot drift space for pion decay and a shielding layer of concrete and steel sufficient to stop muons up to 16 BeV. The detector, 6' x 6' in cross section and 12' long, was enclosed in a steel shield room with 12 inches wall and ceiling thickness in turn surrounded by an anticoincidence shield 8' high, 20' wide, and 16' long, which enclosed the detector and its optical system.

* Based on work performed under the auspices of the U. S. Atomic Commission.

The neutrino flux at the detector was computed using several independently developed computer programs.[6] These programs take into account the focusing of the horn as well as the probability for neutrinos reaching the detector from decays in various parts of the drift space. Measurements of the pion focusing properties of the horn have been reported.[5] The intensity of protons hitting the target was measured by polyethylene and aluminum foil activation and also by a secondary emission detector.[7] These monitors determine the proton intensity to approximately 5%.

The original measurements[8] of the spectrum of angle and momentum for π^+ production have been used to compute the shape of the neutrino spectrum from the beryllium target; however, more recent measurements by Marmer et al[9], Derrick et al[10] and Lundquist and Marmer[11] are in disagreement with the original survey.

For this experiment we have computed the values of the ratios of positive pion fluxes in the original survey to the more recent measurements[9, 11] at 3^o at 1.0, 1.5, 2.0 and 2.5 GeV/c. Using these ratios to reweigh the 0.4, 0.6, 0.8 and 1.0 GeV/c neutrino flux gives an average overall increase in the neutrino flux of 1.5. This inexact procedure based on incomplete data does not allow us to claim knowledge of the absolute flux to better than ± 30%. Final determination of the neutrino flux must await new measurements of the π^+ production cross-section from beryllium.

Figure 2a shows the corrected neutrino spectrum.

The detector consisted of 66 half-inch thick steel plates, 66 two-gap spark chambers, and 22 plastic scintillator sheets.[3] The spark chambers were photographed via a series of 66 mirrors, one for each spark chamber producing a cylindrical Fresnel lens. In addition to the stereo spark chamber cameras, a third camera recorded from a four trace oscilloscope display the rf structure of the beam, the presence of any pulse from the cosmic ray anticoincidence shield, and any sig-

nals from each of the scintillator sheets in the detector. The trigger signal for the spark chamber electronics was the presence of a pulse in any two sequential scintillator sheets during a gated on time of 100 microseconds. This requires a minimum particle range of 40 gm/cm^2. The rate of triggering primarily due to accidental cosmic ray events is about one in every fifteen machine pulses. The rate of neutrino triggers was approximately one in every two hundred pulses.

During the four one week runs, the machine intensity averaged 10^{12} protons/pulse and a total of 3×10^{17} protons were extracted onto the target. The total neutrino trigger rate was approximately 200 events per day for a total of 6,000 neutrino triggers. Half of these triggers were due to events originating outside the detector volume.

The film was double scanned to select events with vertices inside the detector fiducial volume with 95% efficiency. The events observed were 80% single track, 15% 2 prong and 5% $>$ 2 prong or with showers present. The distribution of events throughout the detector volume was uniform as expected for weakly interacting neutral particles. The fiducial volume limits were 2 inches from the chamber edges. No edge effects were observed. The number of scattering ($>10^{\circ}$) of the single prong events gives a limit of less than 3% strongly interacting particle content. Hence, the tracks were taken to be muons.

Accepted for the "elastic" sample were all single track stopping events and all 2 prong stopping events which could fit an elastic event allowing generously for the range of Fermi motion. This sample contained 90% single tracks and 10% 2 prong events. There was also an additional criteria of a minimum muon momentum of 300 MeV. This allowed additional discrimination against inelastic events as well as limiting the events to the region in which the neutrino spectrum was known.

In order to correct these events to the total production rate, an average stopping probability for muons of various direction and momenta inside the detector was

computed. Each event was then assigned a statistical weight corresponding to the inverse of the stopping probability.

We have used the cross-section ratios and inelastic cross-section shapes given by Berman and Veltman[12] to predict a total inelastic contribution of 30% for the ZGS neutrino spectrum. The inelastic channel via N^*_{1236} or higher resonances results in a shift of the muon momentum to lower values. With the 300 MeV/c minimum momentum cutoff and the elimination of obvious multiprong inelastic events there remains a background from this calculation of 10 ± 5% inelastic events in the "elastic" sample. This correction was made as 10% proportional subtraction.

We have alternatively attempted to estimate the number of muons > 300 MeV/c associated with N^* production using measurements from the 1964-1965 CERN Freon (CF_3Br) bubble chamber experiments.[17] We have taken into account the difference in shape of the CERN and revised ANL neutrino spectra in this estimate. In Figure 2b, the background of muons from N^* production would be expected to rise for successively lower values of p_μ down to 300 MeV/c. Events with p_μ of 300 to 400 MeV/c fall predominantly into the low momentum transfer bins, $t < 0.1$ $(BeV/c)^2$, on the distributions shown in Figure 3b and 3c. This may provide an explanation of the excess low momentum transfer events. This estimate would give an upper limit of 20 to 25% inelastic events rather than 10%.

The difference in our two estimates arises principally from the shapes of the rise of the inelastic total cross-section with neutrino energy in the region of threshold to 1.0 GeV, as given in references 12 and 17.

Figure 2b shows a plot of the weighted observed muon spectrum in all single track stopping events. The curve is the calculated elastic muon spectrum for a typical form factor, $M_{A_1} = 0.8$ GeV. Inclusion of nuclear effects has little effect on this spectrum shape which principally reflects the neutrino spectrum shape in this forward angular region. The calculated muon spectrum from elastic inter-

actions fits the observed data above 300 MeV/c. The excess of low energy muons below 300 MeV is presumably associated with N^* production.

The incident neutrino energy can be calculated for each event from the muon momentum vector if the target neutron is at rest:

$$P_\nu = \frac{E_\mu - m_\mu^2/2m_p}{1 - \frac{1}{m_p}(E_\mu - p_\mu \cos\theta_{\mu\nu})}$$

This expression can be used with less than 10% error for the case where Fermi motion is present for muons produced at forward angles $\theta_\mu < 70^\circ$. The event rate combined with the neutrino spectrum gives $\sigma(p_\nu)$ shown in Figure 3a. The solid curves are calculated using a double pole axial vector form factor and the dotted curves are for a single pole case described in equation (5) below.

For interaction with a nucleon at rest the momentum transfer

$$t = -q^2 = \frac{r_\mu^2 - 2E_\mu(E_\mu - p_\mu \cos\theta_{\mu\nu})}{1 - \frac{1}{m_p}(E_\mu - p_\mu \cos\theta_{\mu\nu})} \qquad (1)$$

At small angles

$$t \approx -p_\mu^2 \theta_\mu^2 \qquad (2)$$

and the kinetic energy of the final nucleon

$$E_K \approx t/2m_p. \qquad (3)$$

We calculate the "effective momentum transfer" for our events, t_{eff}, using Eq. 1 and compare this distribution with theory[13] by folding in the ZGS neutrino spectrum and desired nuclear model by Monte Carlo method (see Loevseth[13]).

The nuclear momentum distribution in the nucleus has little effect on the momentum transfer calculation in this forward production region.[1]

The number of events predicted are related to the cross section by

$$\frac{dN}{dt} = N_p N_T \int \frac{d\sigma}{dt} N(p_\nu)\, dp_\nu = N_p N_T N_\nu \frac{d\bar{\sigma}}{dt}$$

where N_p is the number of beam protons (3×10^{17}), N_T is the number of target neutrons per cm^2 in the detector fiducial volume (2.7×10^{26}), and N_ν is the average number of neutrinos passing through the fiducial volume per incident beam proton onto the horn target (2.4×10^{-3}).

The observed cross sections per neutron in the detector fiducial volume are shown in Figure 3b. The errors are computed from event statistics, and do not include the uncertainty in neutrino flux. Figure 3c shows the data in the small momentum transfer region, $0 < t < .2$ $(Bev/c)^2$. The solid lines on Figure 3b, c are the theoretical cross sections for a free neutron target and for bound neutrons in the Fermi gas approximation, ($P_f = 270$ Mev/c).

The shape indicated by the experimental data is close to that of the free neutron cross section. A χ^2 fit of this data to the free neutron cross section using vector form factors of the form

$$G_E(t) = \frac{1}{4.71} G_m(t) = \left(\frac{1}{1 - t/M_\nu^2} \right)^2 \qquad (4)$$

and taking the value $M_\nu^2 = 0.71$[14] and an axial vector form factor

$$F_{A_n} = \left(\frac{1}{1 - t/M_{A_n}^2} \right)^n \quad , \quad n = 1 \text{ or } 2 \qquad (5)$$

yields

$$M_{A_1} = 0.7 \pm .15 \text{ Bev.}$$

and

$$M_{A_2} = 1.05 \pm .2 \text{ Bev.}$$

These two choices of one parameter form factors give two different shapes and asymptotic behaviors for interpretation of experiment. Roughly, $M_{A_2} \sim \sqrt{2}\, M_{A_1}$ provided the fit is to data with $t < M_A^2$.

The absence of large nuclear effects at energy transfer comparable and smaller than nuclear binding energies was unexpected.[15, 16]

We would need a more detailed knowledge of the inelastic cross-sections below neutrino energy of 1 GeV to interpret this result.

We wish to express our appreciation to the operating crews and the staff of the Argonne Particle Accelerator Division who achieved the high beam intensity essential for this experiment and the High Energy Physics technicians and staff of many divisions at Argonne who were involved in the construction and operation of the apparatus. We would like to especially acknowledge the assistance of F. Onesto, H. Vogel, D. Drobnis, and R. Niemann and the important contributions of D. D. Jovanovic, R. C. Lamb, R. A. Lundy and V. L. Telegdi in the preparation and running of the experiment, A. F. Stehney and E. P. Steinberg for the proton beam intensity calibration, and J. Asbury in the data analysis. Also, we would like to thank G. Marmer for communication of his results[11] prior to publication and C. N. Yang, N. Byers, Y. P. Yao and J. Loevseth for many helpful discussions during the course of this experiment and the data analysis.

REFERENCES

(1) T. B. Novey, Proc. Roy. Soc. A301, 113 (1967).

(2) V. L. Telegdi, International Conference on Fundamental Aspects of Weak Interactions, BNL 837 (1963), p. 170.

(3) T. B. Novey, Informal Conference on Experimental Neutrino Physics, CERN 65-32 (1965), p. 31.

(4) S. Suwa and A. Yokosawa, Nucl. Instr. and Meth. 52, 277 (1967).

(5) H. Vogel, W. Brunk, E. Roberts, F. Markley, I. Pollack, H. Hintenberger, V. L. Telegdi, R. Winston, Proceedings of the International Symposium on Magnet Technology, SLAC (1965), pp. 650-6.

(6) A. Aesner and Ch. Iselin, Program Decay, CERN Report 65-17, D. D. Jovanovic, L. R. Thebaud and C. Smith; R. Winston; Y. Cho: Program Bullseye, private communication.

(7) A. F. Stehney and E. P. Steinberg, Nucl. Phys. B5, 188 (1968).

(8) R. A. Lundy, T. B. Novey, D. D. Yovanovitch, and V. L. Telegdi, Phys. Rev. Letters 14, 504 (1965).

(9) G. J. Marmer, K. Reibel, D. M. Schwartz, A. Stevens, T. A. Romanowski, C. J. Rush, P. R. Phillips, E. C. Swallow, R. Winston, and D. Wolf, Argonne National Laboratory, HEP 6801, and Phys. Rev. Letters (to be published).

(10) J. G. Asbury, Y. Cho, M. Derrick, L. G. Ratner, T. P. Wangler, A. D. Krisch and M. T. Lin ANL/HEP 6820.

(11) G. J. Marmer and D. E. Lundquist (private communication).

(12) S. Berman and M. Veltman, Nuovo Cimento 38, 993 (1965).

(13) T. D. Lee and C. N. Yang, Phys. Rev. 126, 2239 (1962); F. Chilton, Nuovo Cimento 31, 447 (1964); J. Loevseth, Phys. Letters 5, 199 (1963).

(14) See e. g. G. Weber Proceedings of the 1967 International Symposium on Electron and Photon Interactions at High Energy, Stanford 1967, pp. 59.

(15) V. L. Telegdi, private communication; S. Berman, CERN 61-22 (unpublished)

B. Goulard and H. Primakoff, Phys. Rev. 135, B1139 (1964).

(16) C. W. Kim and M. Ramm, Phys. Rev. Lett. 20, 35 (1968).

(17) E. C. M. Young, CERN 67112, April 21, 1967.

FIGURE CAPTIONS

Fig. 1 Top and side views of the ZGS neutrino experiment.

Fig. 2 a) Neutrino spectrum with the magnetic horn at 0 and 150 kiloamperes.
b) Muon spectrum, observed elastic events. The solid curve is calculated from the theoretical cross section and the neutrino spectrum shape.

Fig. 3 a) Measured neutrino elastic cross sections and calculated cross sections for two types of axial vector form factors.
b) Comparison of observed $d\sigma/dt$ with cross sections predicted on free neutrons and neutrons in a Fermi gas distribution, P_F = 270 MeV/c.
c) Same as b) with expanded t scale.

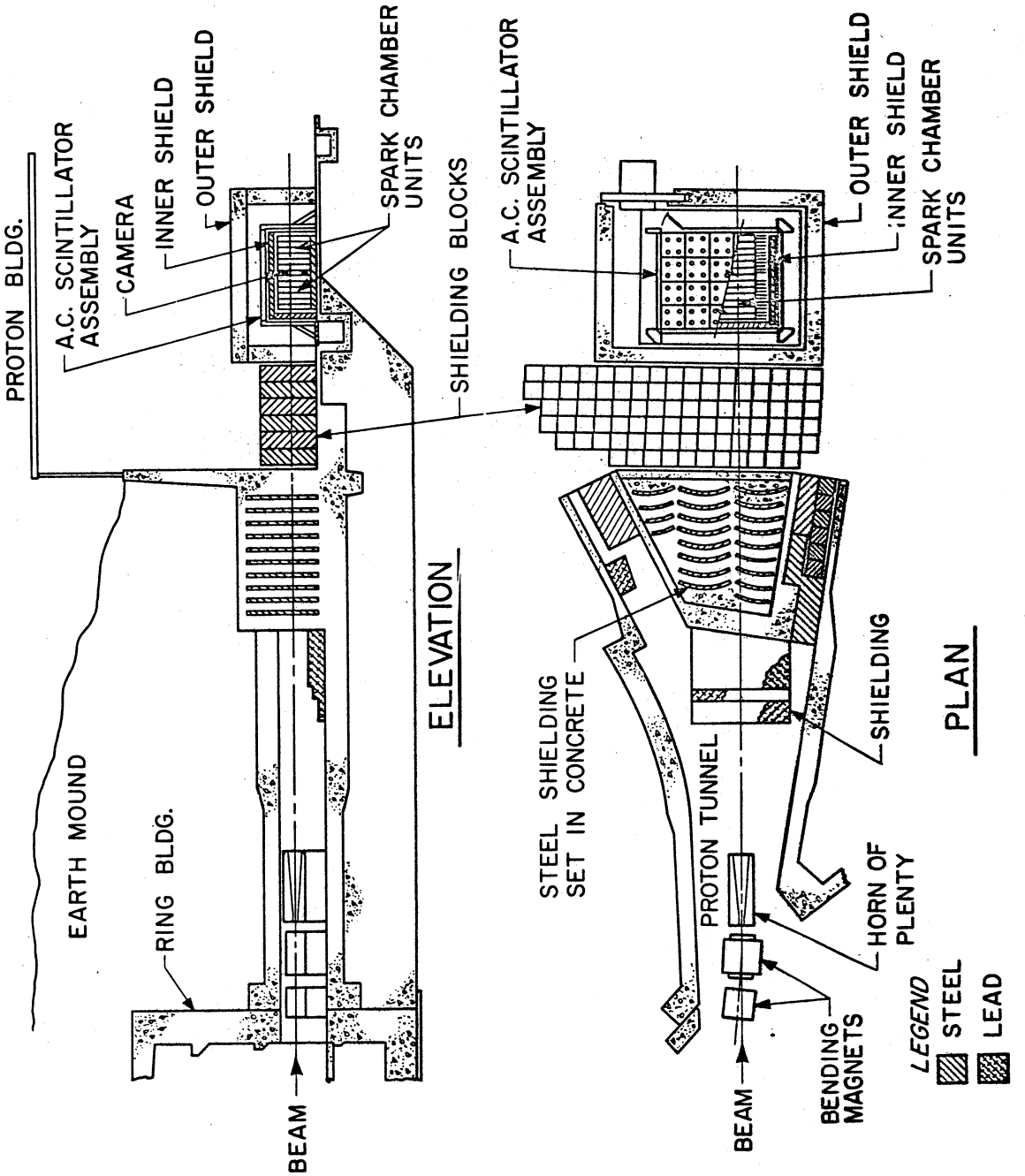
PROTON BLDG.
A.C. SCINTILLATOR ASSEMBLY
CAMERA
INNER SHIELD
OUTER SHIELD
SPARK CHAMBER UNITS
SHIELDING BLOCKS
EARTH MOUND
RING BLDG.
BEAM
ELEVATION
A.C. SCINTILLATOR ASSEMBLY
OUTER SHIELD
INNER SHIELD
SPARK CHAMBER UNITS
STEEL SHIELDING SET IN CONCRETE
PROTON TUNNEL
SHIELDING
HORN OF PLENTY
BENDING MAGNETS
BEAM
PLAN
LEGEND
STEEL
LEAD

Fig. 1

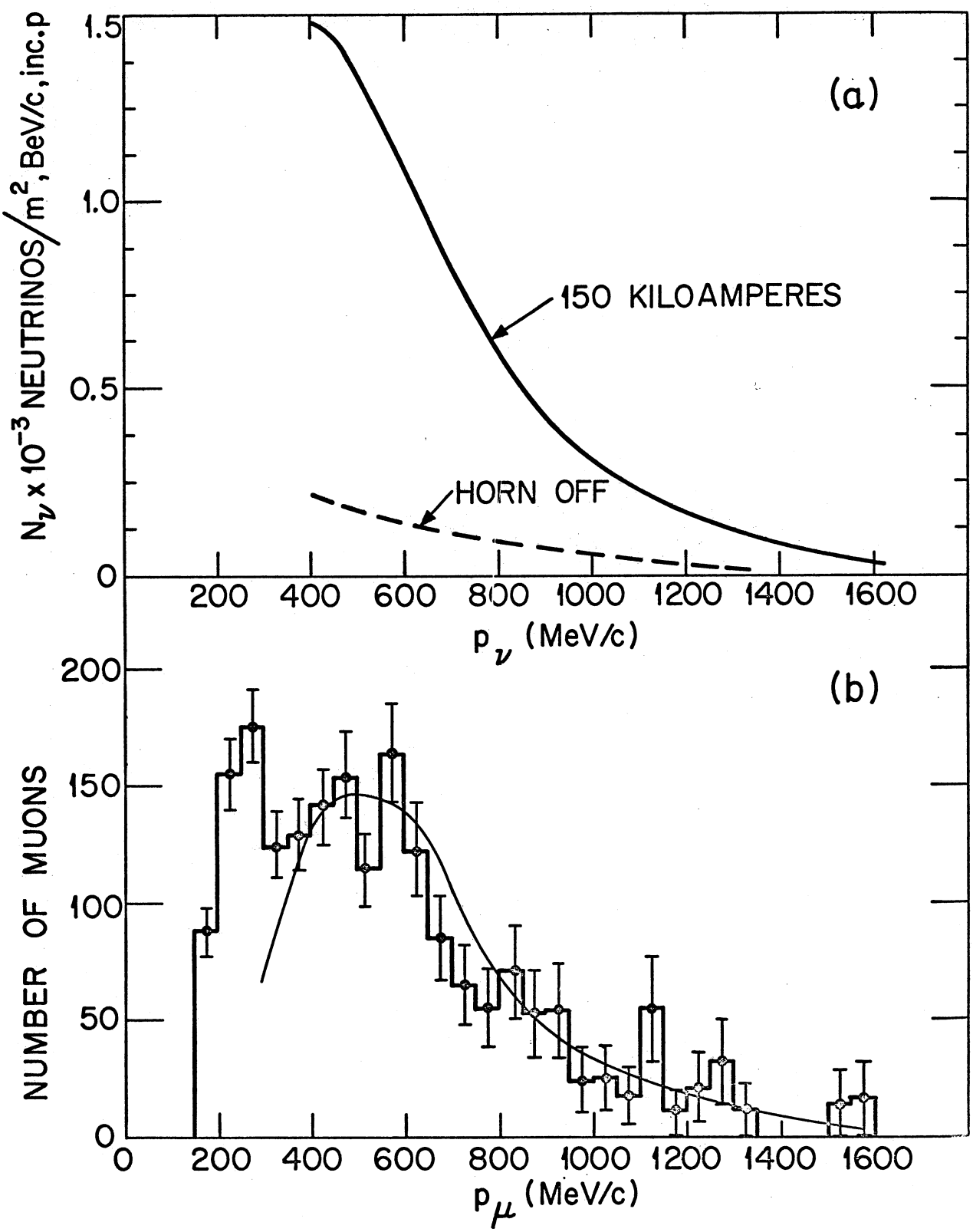
(a)
150 KILOAMPERES
HORN OFF
$N_\nu \times 10^{-3}$ NEUTRINOS/m^2, BeV/c, inc.p
1.5
1.0
0.5
0
200 400 600 800 1000 1200 1400 1600
p_ν (MeV/c)
(b)
NUMBER OF MUONS
200
150
100
50
0
0 200 400 600 800 1000 1200 1400 1600
p_μ (MeV/c)

Fig. 2

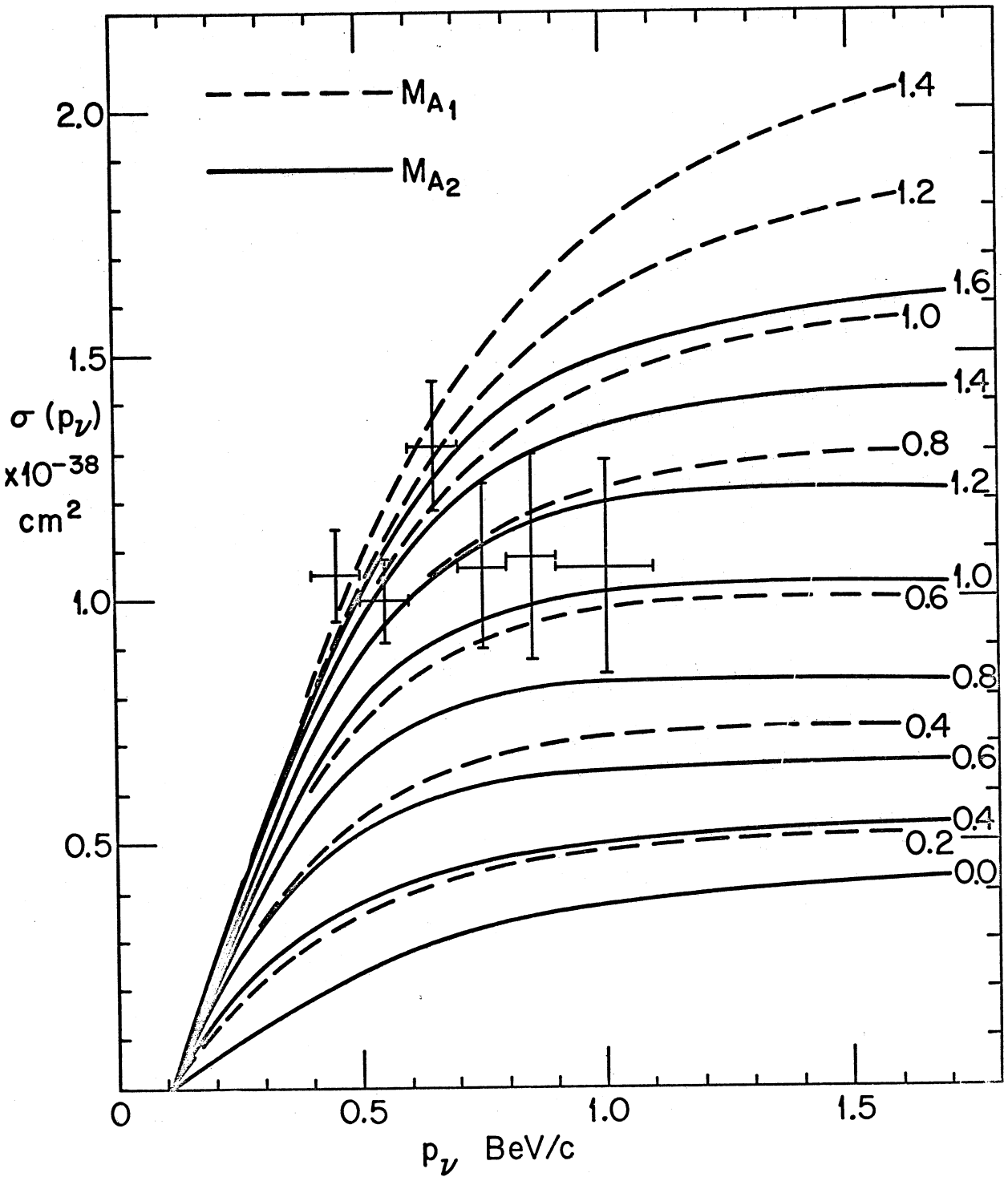
M_{A_1}
M_{A_2}
1.4
1.2
1.6
1.0
1.4
0.8
1.2
1.0
0.6
0.8
0.4
0.6
0.4
0.2
0.0
2.0
1.5
1.0
0.5
$\sigma(p_\nu)$
$\times 10^{-38}$
cm^2
0
0.5
1.0
1.5
p_ν BeV/c

Fig. 3a

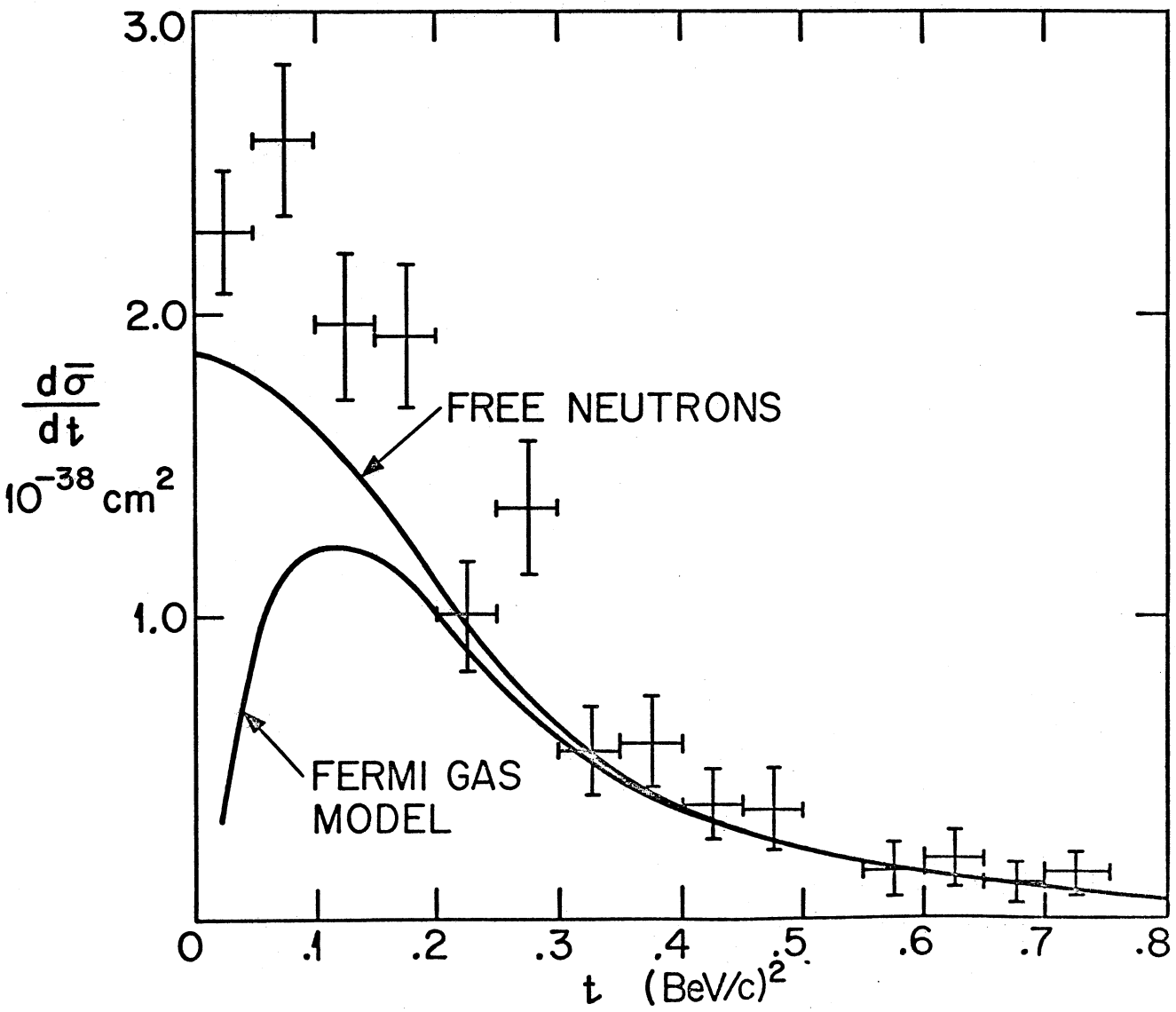
3.0
2.0
1.0
$\frac{d\bar{\sigma}}{dt}$
10^{-38} cm^2
FREE NEUTRONS
FERMI GAS
MODEL
0
.1
.2
.3
.4
.5
.6
.7
.8
t (BeV/c)^2

Fig. 3b

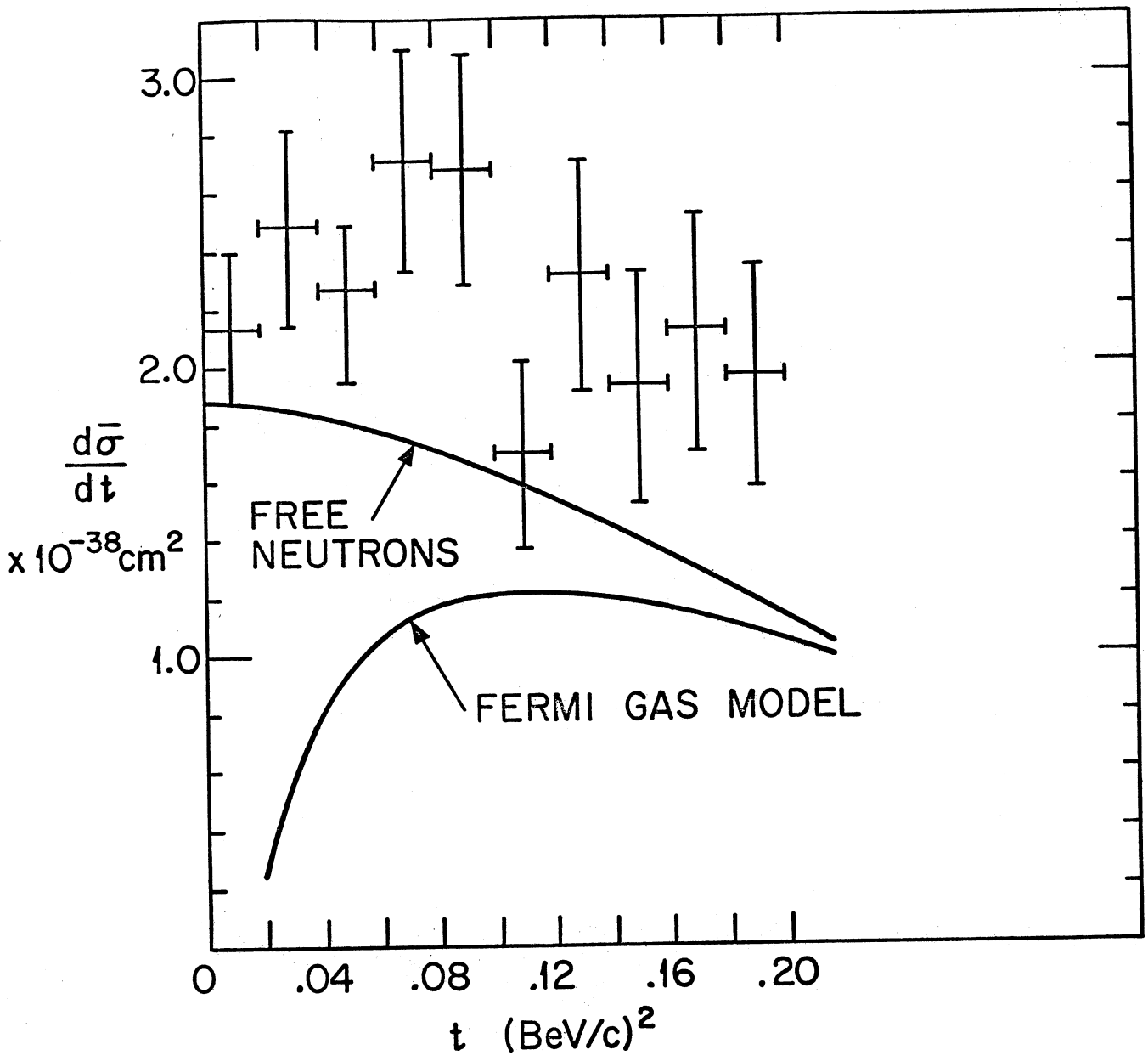
3.0
2.0
1.0
$\frac{d\bar{\sigma}}{dt}$
$\times 10^{-38} cm^2$
FREE
NEUTRONS
FERMI GAS MODEL
0
.04
.08
.12
.16
.20
t (BeV/c)^2

Fig. 3c